*Int. J. Electrochem. Sci.*, 8 **(2013)** 3441 - 3453

International Journal of
ELECTROCHEMICAL
SCIENCE
www.electrochemsci.org

# Effect of $CO_2$ Saturation on the Corrosion Behaviour of AZ31B Magnesium Alloy in $Na_3PO_4$ Solutions

*Wei Bai*[*], *Jinmiao Yu, Yan Yang, Yanqing Ye, Junming Guo, Yingjie Zhang*

The Engineering Laboratory of Polylactic Acid-Based Functional Materials of Yunnan, Yunnan University of Nationalities, Kunming 650092, China
[*]E-mail: bw369852147@qq.com

*Received:* 25 January 2013 / *Accepted:* 20 February 2013 / *Published:* 1 March 2013

Effect of $CO_2$ saturation on the corrosion behaviour of AZ31B magnesium alloy in the presence of different concentrations of $Na_3PO_4$ solution was investigated by open circuit potential (OCP), potentiodynamic polarization and electrochemical impedance spectroscopy (EIS). As it was expected, in solution without $CO_2$ the corrosion rate decreases with increasing $Na_3PO_4$ concentration and the passive behaviour of AZ31B magnesium alloy apparently occurs when the concentration of $Na_3PO_4$ is increased to $10^{-2}$ mol $L^{-1}$ after 2 h immersion. However, in solution saturated with $CO_2$ the corrosion rate decreases with increasing $Na_3PO_4$ after 2 h immersion. And the corrosion rate in $Na_3PO_4$ solution saturated with $CO_2$ is bigger than that in single $Na_3PO_4$ solution, showing that $CO_2$ obviously accelerates the corrosion of AZ31B magnesium alloy in $Na_3PO_4$ solutions. The corrosion rate is also observed with immersion time decreased in $Na_3PO_4$ solution saturated with $CO_2$ as a result of increase in pH value with time going on.

**Keywords:** Corrosion; AZ31B magnesium alloy; $Na_3PO_4$; $CO_2$

## 1. INTRODUCTION

Nowadays, magnesium alloys have received extensive application in the aerospace, automotive application and electronic industries because of their excellent physical properties, including low density, high strength to weight ratio, excellent electrical conductivity, high thermal conductivity and good electromagnetic shielding characteristics among others [1-3]. However, the magnesium alloy has a low corrosion potential and easily corrodes, which limits its extensive utilization in these fields. Therefore, corrosion behaviour of magnesium and its alloy have been widely investigated in various environments and is still a significant research field [4-11].

Many material and components made by magnesium alloy are usually exposed to atmosphere containing abundant vapor and $CO_2$. It is easy to form a thin film saturated with $CO_2$ on the surface of magnesium alloy in this environment where magnesium alloy is active and easily corroded. Therefore, $CO_2$-induced atmospheric corrosion of magnesium and its alloys has received the attention of many researchers [8-11]. It is also reported that $CO_2$ may play an important role in the corrosion of magnesium alloy. For examples, Baril et al [8] studied the corrosion of pure magnesium in $Na_2SO_4$ solution aerated and deaerated. Their results showed that $O_2$ did not influence the corrosion of magnesium and the corrosion rate of magnesium was controlled by $HCO_3^-$ concentration in the presence of $CO_2$. Lin et al [9] also studied the role of $CO_2$ in the initial atmospheric corrosion of AZ91 magnesium alloy in the presence of NaCl. NaCl was added by spraying the sample with saturated NaCl solution in 90% ethanol and the volume of $CO_2$ in mixed gas was 1%. They suggested NaCl-induced corrosion was inhibited in the presence of $CO_2$ by the formation of slightly soluble corrosion products containing hydroxy carbonates and hydroxy chlorides that provided a partly protective layer on the surface of the magnesium alloy. But it is unlikely to form a thin fluid film on magnesium alloy in their study. While Lindström et al. [10] made investigations of the influence of carbon dioxide on the atmospheric corrosion of magnesium; they concluded that in the presence of 350 ppm $CO_2$ the corrosion rate was only 25% of that registered in $CO_2$-free air. This was explained by the formation of a protective carbonate layer. Qu et al. [11] investigated the corrosion behaviour of AZ31B magnesium alloy in different concentrations of NaCl solution saturated with $CO_2$, they showed that the presence of $CO_2$ accelerated the anodic dissolution in NaCl solution. However, little has been studied about the corrosion mechanism of magnesium alloy in the presence of other salts saturated with $CO_2$.

Considering that metal phosphates are insolubility in neutral water and have high temperature resistance and chemical stability [12], phosphate chemical conversion may be a promising coating method for corrosion protection films of magnesium alloys. More and more researchers have interests in studying effect of phosphates on the corrosion of magnesium alloys [12-16]. Previous studies concerning the electrochemical performance of AZ91D alloy in phosphate electrolytes dealt mainly with producing a film by chemical [13] or electrochemical [14] oxidation to form protective coatings on AZ91D substrate. Niu et al. [15] succeeded in forming a zinc phosphate coating on AZ91D alloy with a typical phosphate microstructure having better corrosion resistance due to the presence of crystalline zinc in the coat. Heakal et al. [16] studied the influence of pH on the corrosion behavior of Mg-based AZ91D alloy in a constant composition phosphate medium, they suggested that pH value of phosphate medium have an important effect and spontaneously formed protective layers on the AZ91D surface greatly improve with increasing pH value of phosphate (over 8.1), which leads to partial blocking of the film pores; their results also showed the corrosion rate in $NaH_2PO_4$ solution is far larger than that in $Na_3PO_4$ solution. But literature available to date about effect of the concentration of phosphate on the corrosion of magnesium alloy with and without $CO_2$ is scare. Consequently, there is no clear understanding of the role of $CO_2$ in the corrosion kinetics of magnesium alloy in $Na_3PO_4$ solution saturated with $CO_2$.

The purpose of the present study is to study the detailed reaction sequence of AZ31B alloy in $Na_3PO_4$ solutions saturated with and without $CO_2$ by open circuit potential (OCP), potentiodynamic

polarization and electrochemical impedance spectroscopy (EIS) and is to discuss the effect of $CO_2$ saturation on the corrosion mechanism of magnesium alloy in $Na_3PO_4$ solutions.

## 2. EXPERIMENTAL METHODS

### *2.1 Materials*

The experiments were performed with AZ31B magnesium alloy specimens with the following chemical composition (wt %): Al 3.05 %, Zn 0.99 %, Mn 0.28 %, Fe 0.003 %, Si 0.025 %, Cu 0.002 %, Ni 0.0049 % and Mg balance.

Sodium phosphate ($Na_3PO_4$) was of analytical grade. Different concentrations of $Na_3PO_4$ (0, $10^{-5}$, $10^{-4}$, $10^{-3}$, $10^{-2}$, $10^{-1}$ mol $L^{-1}$) were prepared from distilled water. The experimental solution was aerated using a $CO_2$ gas generator. pH was surveyed by PHS-25 pH-metre.

### *2.2 Electrochemical measurements*

The working electrode was embedded in a PVC holder using epoxy resin given an exposed surface of 4.0 $cm^2$. The exposed face was abraded with emery paper from 100 to 1200 grades, scoured with distilled water, degreased with acetone, washed again with distilled water, and dried with a blower.

A three-electrode system including a working electrode, an auxiliary electrode and a reference electrode was used for electrochemical measurements in 250 mL solution. Auxiliary electrode was a platinum foil and the reference electrode was a saturated calomel electrode (SCE) with a Luggin capillary positioned close to the working electrode surface in order to minimize ohmic potential drop. The working electrodes were immersed in the test solution at 30℃ for 2 h before measurement until a steady state appeared. All electrochemical measurements were carried out using a PAR 2263 Potentistat/Galvanostat (Princeton Applied Research). EIS was carried out in a frequency range of $2\times10^6$ Hz to 0.1 Hz using a 10 mV peak-to-peak voltage excitation. The potentiodynamic polarization scan was carried out by polarizing from -1.9 V to 1.0 V with respect to the free corrosion potential ($E_{corr}$ vs. SCE) at a scan rate of 1 mV $s^{-1}$. Each experiment was repeated at least three times to check the reproducibility.

## 3. EXPERIMENTAL RESULTS

### *3.1 Solution saturated with $CO_2$*

It is generally agreed that the following reactions will occur in solution containing $CO_2$:

$$CO_2(g)\rightarrow CO_2(aq) \quad (1)$$

$$CO_2(aq)+H_2O \rightarrow H_2CO_3(aq) \rightarrow H^+(aq)+HCO_3^-(aq) \quad (2)$$

$$HCO_3^-(aq) \rightarrow H^+(aq)+CO_3^{2-} \quad (3)$$

When $CO_2$ is saturated in the solution, hydrogen ion ($H^+$) will be in equilibrium with $CO_2$, and pH will be steady. So pH value of the solution can be used to determine whether and when the solution is saturated with $CO_2$.

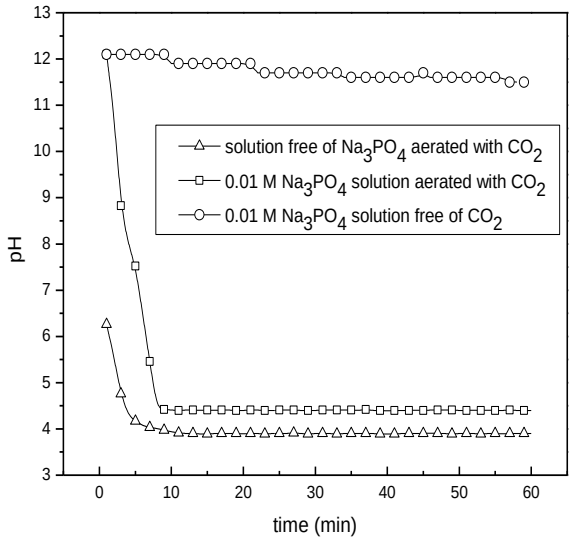


**Figure 1.** pH value of the solution with and without $Na_3PO_4$ as a function of the time aerated with $CO_2$

Fig.1 shows the pH value of the solution with and without $Na_3PO_4$ as a function of the time aerated with $CO_2$ at 30℃. It is evident that, the pH value of the solution with and without $Na_3PO_4$ tends firstly towards negative direction quickly, and then it changes slowly until steady state is established after 10 minutes. Therefore, the solution saturated with $CO_2$ can be obtained after 10 minutes aerated with $CO_2$. So 10 minutes were chosen as the aeration time in this paper.

### *3.2 Electrochemical studies*

#### *3.2.1 Open circuit potential (OCP)*

The OCP experiments of AZ31B in solution saturated with $CO_2$ without and with 0.01 mol $L^{-1}$ $Na_3PO_4$ at 30℃ were recorded and plotted in Fig. 2. As it can be seen, the corrosion potentials ($E_{corr}$ vs. SCE) shift towards positive direction quickly during the initial 2000 s, then slightly increase with time and reach a steady state at 6000 s in solution saturated with $CO_2$ with and without $Na_3PO_4$. Both curves in solution saturated with $CO_2$ with and without $Na_3PO_4$ have similar shapes. Fig.2 also shows that the corrosion potential in $Na_3PO_4$ solution saturated with $CO_2$ is higher than that measured in

solution without $Na_3PO_4$ saturated with $CO_2$ but lower than that in $Na_3PO_4$ solution in the absence of $CO_2$.

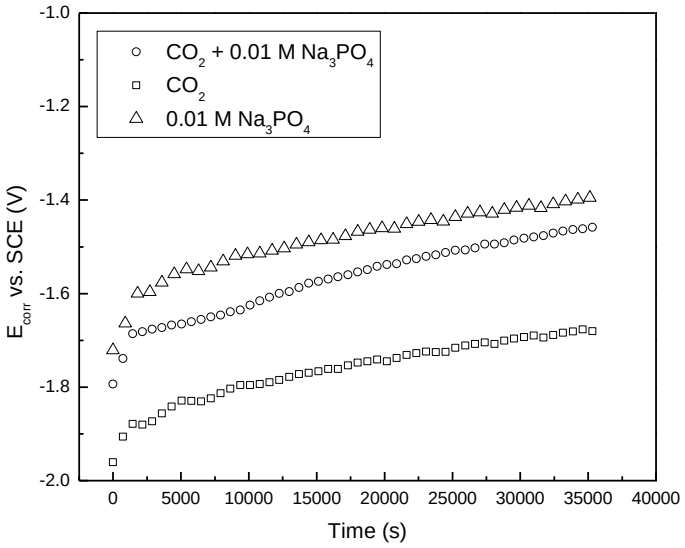


**Figure 2.** Variation of the OCP of AZ31B in solution saturated with $CO_2$ without and with $Na_3PO_4$

This indicates that $Na_3PO_4$ affects the kinetics of the anodic reaction of AZ31B magnesium alloy in solution saturated with $CO_2$ more strongly. Because the OCP does not change obviously with increasing immersion time after 2 h immersion, in this article 2 h was chosen as the immersion time in electrochemical studies.

*3.2.2 Potentiodynamic polarization*

To discuss the effect of $Na_3PO_4$ on the kinetics of the anodic reaction of AZ31B magnesium alloy in solution, the potentiodynamic polarization curves for the corrosion of AZ31B in solution without and with $CO_2$ containing different concentrations of $Na_3PO_4$ at 30 ºC were shown in Fig.3a and b, respectively. Fig.3a shows that, corrosion potentials ($E_{corr}$ vs. SCE) are shifted to noble direction with increasing $Na_3PO_4$ concentration in the absence of $CO_2$, the anodic branches are shifted to more positive potential direction while the cathodic branches dose not change obviously, suggesting that $Na_3PO_4$ mainly retards the anodic reaction. And from Fig.3a it also can be seen that, when the concentration of $Na_3PO_4$ is higher than or equal to $10^{-2}$ mol $L^{-1}$, the anodic current densities become very low and do not change with increasing the applied potential (from corrosion potential to 1.5V). This domain corresponds to an apparent passivation zone. Over the potential region of the passive current zone a steady state is established between the rates of metal dissolution and passive film formation. Therefore, the anodic passive behaviour of AZ31B magnesium alloy apparently occurs when the concentration of $Na_3PO_4$ is increased to $10^{-2}$ mol $L^{-1}$ in the absence of $CO_2$. Whereas a reverse trend about the effect of $Na_3PO_4$ was observed in the presence of $CO_2$ from Fig.3b. Fig3b

shows that the corrosion potential decreases with increasing the concentration of $Na_3PO_4$ from 0 to 0.1 mol $L^{-1}$ in solution saturated with $CO_2$, and that the anodic current densities obviously increase with increasing the concentration of $Na_3PO_4$, suggesting that $Na_3PO_4$ accelerates the anodic dissolution of AZ31B alloy in solution saturated with $CO_2$.

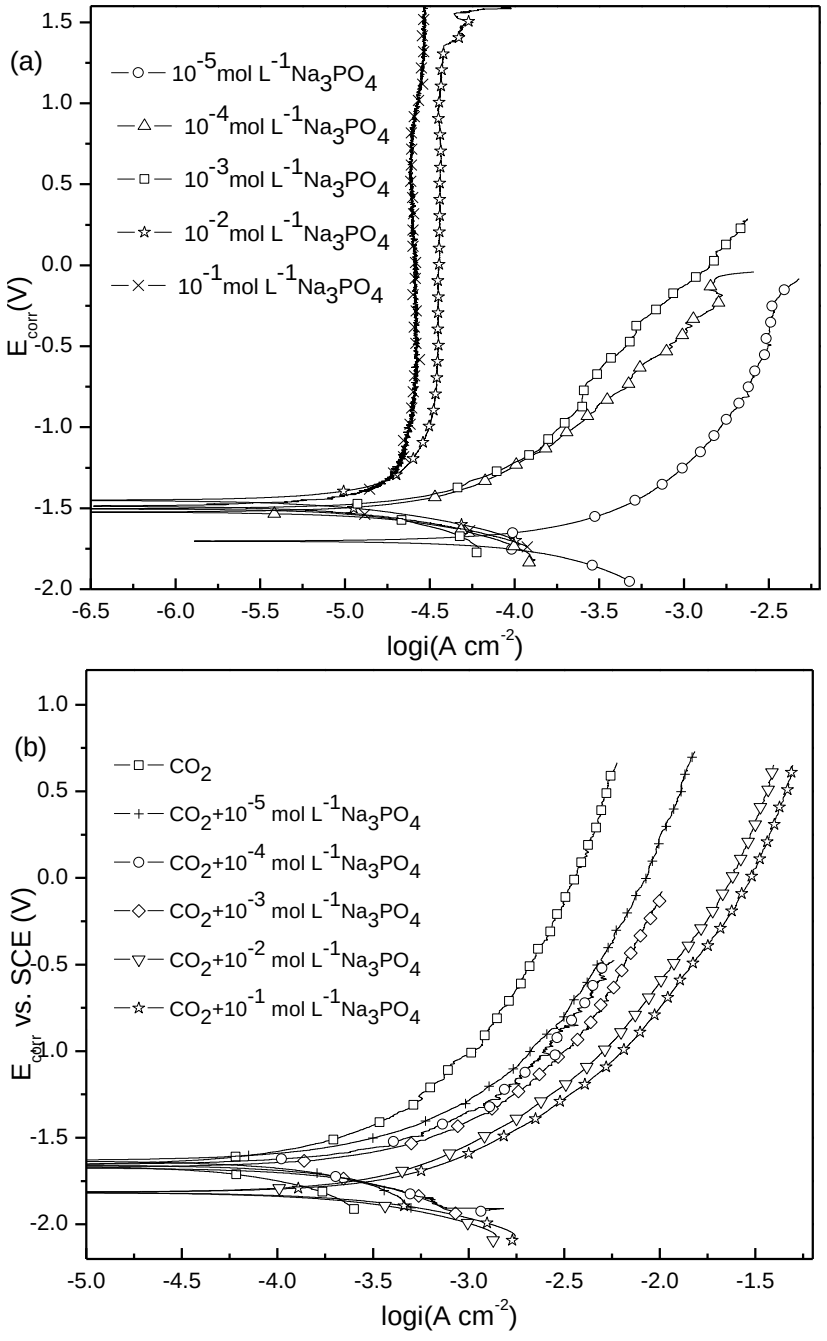


**Figure 3.** Potentiodynamic polarization for magnesium alloy in solution without (a) and saturated with $CO_2$ (b) at different concentrations of $Na_3PO_4$

**Table 1.** Electrochemical parameters from potentiodynamic polarization and EIS in different concentration of $Na_3PO_4$ solution saturated with $CO_2$ at 30 ℃

| $CO_2$ | $C_{Na_3PO_4}$ (mol $L^{-1}$) | $E_{corr}$vs SCE (V) | $i_{corr}$ (μA $cm^{-2}$) | $R_l$ (Ω $cm^2$) | $R_t$ (Ω $cm^2$) | $C_{dl}$ (μF $cm^{-2}$) | $R_f$ (Ω $cm^2$) | $C_{dl}$ (μF $cm^{-2}$) |
|---|---|---|---|---|---|---|---|---|
| 0 | $10^{-5}$ | -1.550 | 112.1 | 256.7 | 1547 | 0.0002 | 1461 | 25.02 |
| | $10^{-4}$ | -1.518 | 56. 3 | 187.0 | 5307 | 0.0005 | 1473 | 24.82 |
| | $10^{-3}$ | -1.504 | 49.9 | 157.4 | 6368 | 0.0006 | 440.0 | 28.03 |
| | $10^{-2}$ | -1.478 | 28.2 | 36. 5 | 14120 | 0.0003 | - | - |
| | $10^{-1}$ | -1.485 | 19.9 | 34.2 | 26240 | 0.00012 | - | - |
| saturation with $CO_2$ | 0 | -1.652 | 125.6 | 346.1 | 562.6 | 0.0007 | 65.39 | 25.50 |
| | $10^{-5}$ | -1.653 | 151.3 | 191.9 | 431.3 | 0.0009 | 181.9 | 18.20 |
| | $10^{-4}$ | -1.629 | 177.8 | 110.8 | 418.6 | 0.0010 | 148.3 | 23.57 |
| | $10^{-3}$ | -1.665 | 251.7 | 58.8 | 315.9 | 0.0016 | 99.68 | 31.47 |
| | $10^{-2}$ | -1.861 | 501.4 | 31.4 | 220.5 | - | - | - |
| | $10^{-1}$ | -1.856 | 512.3 | 29.8 | 219.7 | - | - | - |

The corrosion potential $E_{corr}$ and corrosion current density $i_{corr}$ obtained from these curves were summarized in Table 1. Similar to the results obtained from OCP tests, the corrosion potential in $Na_3PO_4$ solution saturated with $CO_2$ is lower than that in $Na_3PO_4$ solution in the absence of $CO_2$, as shown in Table 1. It also can be seen from Table 1 that, with increasing concentration of $Na_3PO_4$ from 0 to 0.1 mol $L^{-1}$, the $i_{corr}$ values in the presence of saturation $CO_2$ increase from 125.6 to 512.3 μA $cm^{-2}$ while those in the absence of $CO_2$ only decrease from 112.1 to 19.9 μA $cm^{-2}$. The corrosion rate is much higher in solution saturated with $CO_2$ than without $CO_2$ at each same concentration of $Na_3PO_4$. That is to say, $CO_2$ significantly accelerates AZ31B alloy corrosion in $Na_3PO_4$ solutions, which can be attributed to the co-effect of $CO_2$ and $Na_3PO_4$.

### *3.2.3 EIS*

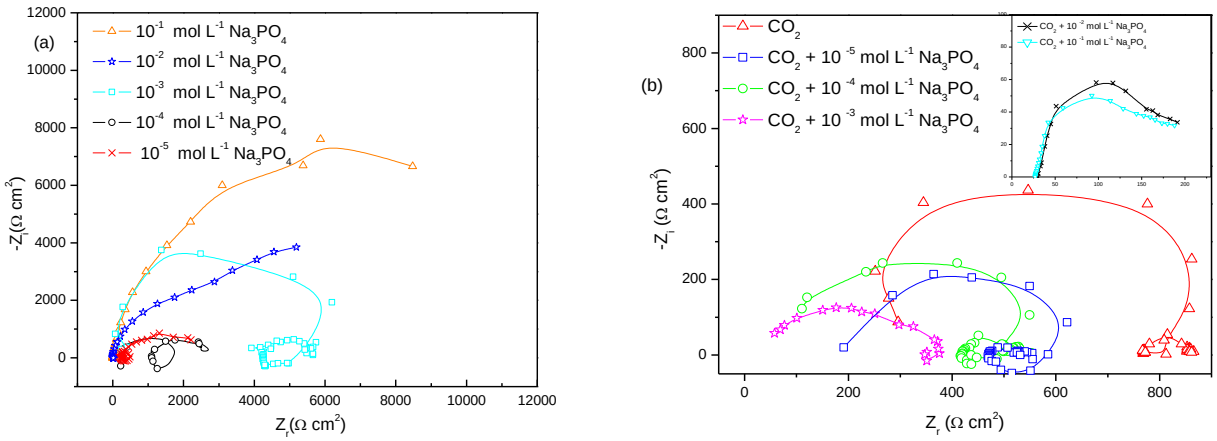


**Figure 4.** EIS of AZ31B at different concentrations of $Na_3PO_4$ solution without (a) and saturated with $CO_2$ (b).

In order to compare the corrosion behaviour of different solutions, Fig. 4a and b show the Nyquist diagrams of AZ31B for different concentrations of $Na_3PO_4$ without and saturated with $CO_2$ at 30℃. It is easy to see from these figures that all impedance spectra are rather complex when the concentration of is lower than $10^{-3}$ mol $L^{-1}$. In general, the EIS for AZ31B is quite similar to that of magnesium and AZ21 in NaCl solution [11,17,18], even though the data is much scattered, the trend is still clear that the EIS consists of three loops, one capacitive in the high frequency range (hf), one inductive loop in the intermediate-frequency range (mf) and another capacitive loop in the low frequency (lf) in low concentration of $Na_3PO_4$. However, the intermediate-frequency inductive loop and low frequency capacitive almost disappear when the concentration is higher than $10^{-3}$ mol $L^{-1}$, correspondingly, the impedance spectra mainly exhibit one capacitive loop. Additionally, when the concentration is higher than $10^{-3}$ mol $L^{-1}$, these capacitive loops in the absence of $CO_2$ only are part of depress semicircles and the diameters are very large comparing to that in solution saturated with $CO_2$, The larger values of impedance and the character of impedance diagrams in the absence of $CO_2$ suggest existence of a passive film on AZ31B magnesium alloy.

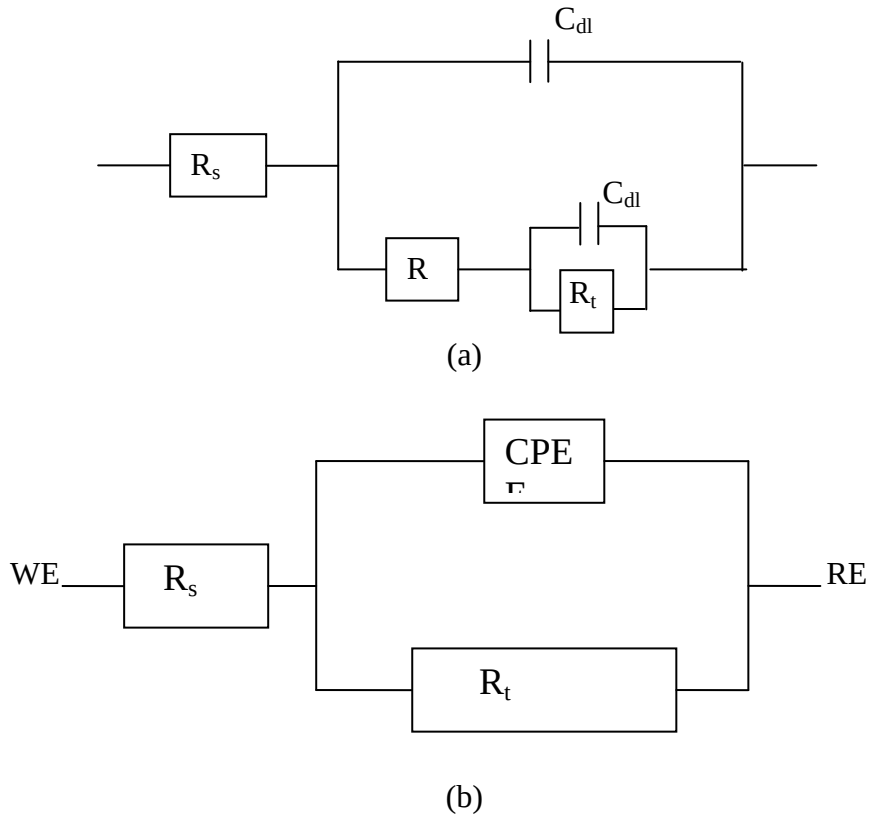


**Figure 5.** Equivalent circuit of EIS in low (a) and high (b) concentration of $Na_3PO_4$

It is generally agreed that the capacitive loop in the high frequency region is always related to the transient resistance ($R_t$) and the double layer capacitance ($C_{dl}$) of the electrode [8,18-21], and it is possible to obtain the oxide film resistance of AZ31B from these loops as presented in Fig.4. Comparing the semicircle of high frequency capacitive loop, it is easy to see that the loop of the

solution saturated with $CO_2$ is smaller than that without $CO_2$ at each concentration of $Na_3PO_4$. With increase of the concentration of $Na_3PO_4$ saturated with $CO_2$ the diameter decreases, meaning that the corrosion of AZ31B accelerates, whereas in the absence of $CO_2$ the corrosion rate decreases with increase of the concentration of $Na_3PO_4$. These results are consistent in potentiodynamic polarization curves.

According to Song et al. [17,18] the low frequency capacitive loop is related to $Mg^+$ ion concentration within the face oxide broken area. The inductive loop in the intermediate-frequency range is generally attributed to the adsorbed species such as $Mg(OH)^+$ or $Mg(OH)_2$ [17,18,22]. According to our observations, the rate of adsorption of these species is only significant in solution containing higher concentration of $Na_3PO_4$ saturated with and without $CO_2$, since there is no inductive loop appeared in higher concentration of $Na_3PO_4$ solutions.

The EIS results were simulated using the equivalent circuit shown in Fig.5a (low concentration) and b (high concentration) to pure electronic models that could verify or role out mechanistic models and enable the calculation of numerical values corresponding to the electrochemical system under investigation [23]. In these circuits, $R_s$ is solution resistance, $R_t$ is charge transfer resistance and $C_{tdl}$ is the double layer capacity associated to the oxidation film of AZ31B; $R_f$ and $C_{fdl}$ are associated to the adsorption film on the oxidation film of AZ31B. In high concentration of $Na_3PO_4$, the equivalent circuit contains inductance $L$ and disturbs resistance; $Q$ is the constant phase element comprising $C_{tdl}$ and $R_t$, $R_s$, $R_t$, $R_f$ and $Q$ are all obtained from EIS in Fig. 4 via equivalent circuit in Fig. 5. And the solid lines in Fig.4 show the fit of the experimental data according to this model circuit. $C_{dl}$ is accounted using the following equation [24]:

$$C_{dl} = \frac{1}{2\pi f_{max} R} \qquad (4)$$

Where $f_{max}$ represents the frequency at which imaginary value reaches a maximum in one capacitive loop in the Nyquist plot. $R$ is the resistance ($R_t$, $R_f$) and $C_{dl}$ the double layer capacity ($C_{tdl}$, $C_{fdl}$). The resistances and double layer capacity ($C_{tdl}$, $C_{fdl}$) are all listed in Table 1.

From Table 1 it can be found, with the increasing concentration of $Na_3PO_4$ without $CO_2$, that $C_{tdl}$ value decreases and $R_t$ values increase, which reveals that corrosion rate of AZ31B decreases with increasing concentration of $Na_3PO_4$; while with the increasing concentration of $Na_3PO_4$ saturated with $CO_2$, the results are the contrary. The $R_t$ values are far smaller in solution saturated with $CO_2$ than single $Na_3PO_4$. But $C_{tdl}$ values are just the opposite. That is, the corrosion rate increases markedly in the solution aerated with $CO_2$. These results are well in agreement with the results obtained from potentiodynamic polarization.

### *3.2.4 Effect of immersion time*

To further investigate the effect of immersion time on the corrosion of AZ31B in $Na_3PO_4$ solution saturated with $CO_2$, the potentiodynamic polarization curves and EIS of $10^{-2}$ mol $L^{-1}$ $Na_3PO_4$

solution saturated with $CO_2$ at different time are presented in Fig 6a and b, respectively. Fig 6a shows that the corrosion potentials shift to more positive direction with increasing immersion time, the anodic branches are shifted to more positive potential direction, indicating that the anodic dissolution is retarded with increasing immersion time.

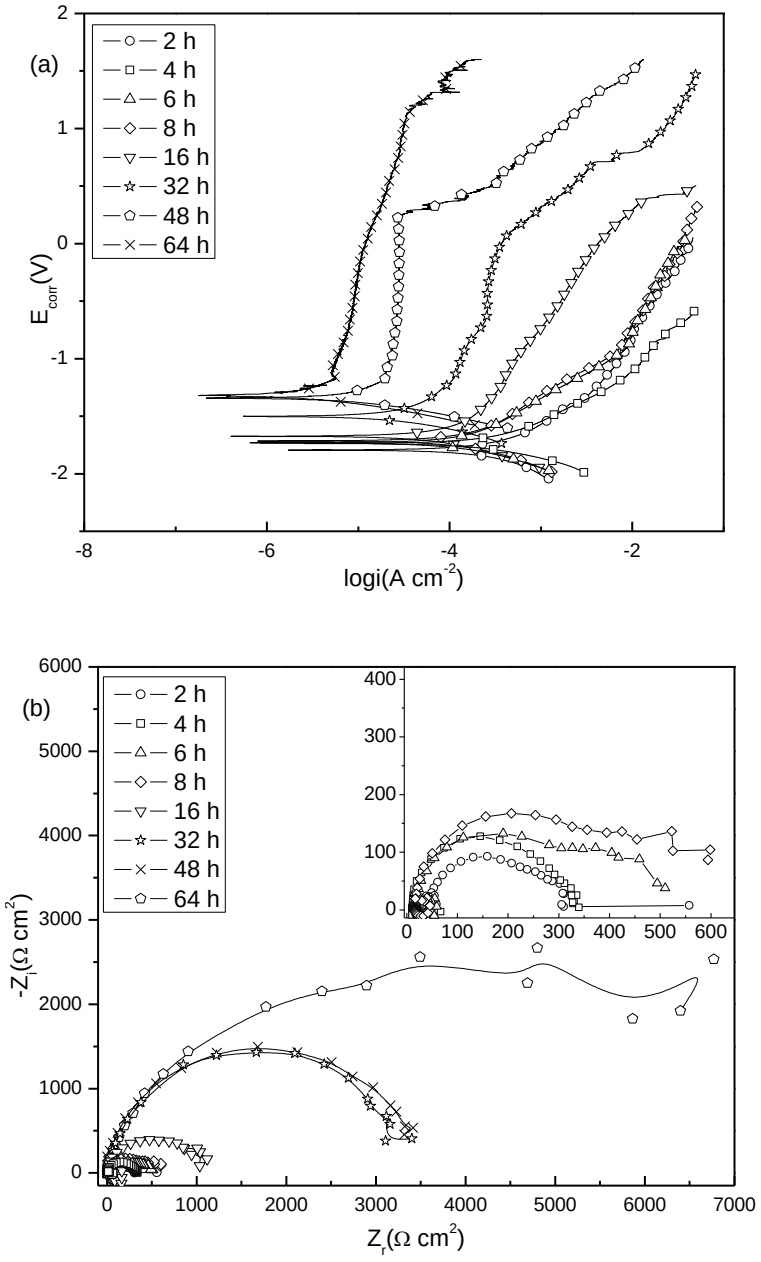


**Figure 6.** Potentiodynamic polarization (a) and EIS (b) of AZ31B in solution saturated with $CO_2$ in the presence of $10^{-2}$ mol $L^{-1}$ $Na_3PO_4$ at different times

As a result, the corrosion current also decreases with increasing immersion time. From these polarization curves, it is also clear passive behaviour will occur if the immersion time is longer than 32 h, and the passive range increases with increasing immersion time. It also can be seen from Fig. 6b

that, the immersion time increases significantly the size of the capacitive loop, when the time is raised to 32 h, the diameter of the capacitive loop becomes very large, and the capacitive loop increases more obviously than that before 32 h, the larger values of impedance and the character of impedance diagrams suggest existence of a corrosion film in $Na_3PO_4$ solution saturated with $CO_2$ after immersion for 32 h. And the film becomes more protective with increasing immersion time. This fact is consistent with the result from Baril et al. [8]. Baril also have reported that the concentration of $HCO_3^-$ is a main factor of corrosion rate and in aerated solution the magnesium surface is covered with a porous film (MgO, $Mg(OH)_2$) which became thicker with time and had a low protective action.

## 4 DISCUSSION

### *4.1 Corrosion in $Na_3PO_4$ solution without $CO_2$*

It is well known that dissolution of magnesium in aqueous solutions proceeds by reduction of water molecules to produce magnesium oxide and/or hydroxide and hydrogen gas.

In $Na_3PO_4$ solution without $CO_2$, $PO_4^{3-}$ will hydrolyze and lead to increase in pH of the solution which brings into strongly alkaline solution. As shown in Fig.1 that pH value of 0.01 M $Na_3PO_4$ is higher than 11.

The anodic dissolution of magnesium in alkaline solution is

$$Mg(s) \rightarrow Mg^+(l) + e \quad (5)$$

$$Mg^+(l) + H_2O \rightarrow Mg^{2+}(l) + OH^-(l) \quad (6)$$

$$Mg(s) + 2OH^-(s) \rightarrow Mg(OH)_2(s) + 2e^- \quad (7)$$

And the corresponding cathodic reaction is

$$2H_2O + 2e^- \rightarrow H_2(g) + 2OH^-(aq) \quad (8)$$

Therefore, countless electrochemical cells begin to form on the surface of AZ31B. Then cations, e.g. $Na^+$, $Mg^+$ will migrate towards to the cathodic areas, at the same time anions, e.g. $PO_4^{3-}$, $OH^-$ will migrate towards to the dissolution sites. Accordingly, insoluble $Mg_3(PO_4)_2(s)$ and $Mg(OH)_2(s)$ will form close to the anodic sites. The anodic dissolution is subsequently retarded. With increase in concentration of $Na_3PO_4$, pH becomes higher, and insoluble $Mg_3(PO_4)_2(s)$ and $Mg(OH)_2(s)$ come into being more easily. Thus the anodic dissolution becomes more difficult. When the concentration of $PO_4^{3-}$ is equal to or higher than $10^{-2}$ mol $L^{-1}$, the insoluble film becomes thicker and more protective; it will exhibit existence of a passive film in electrochemical tests. The phenomena are well in agreement with the results obtained from potentiodynamic polarization and EIS.

However, when in solution saturated with $CO_2$, on the one hand, the formation of $H^+$ and $CO_3^{2-}$ will enhance the conductivity and acidity of the electrolyte rather quickly, the cathodic hydrogen evolution becomes more facile. Accordingly, the corrosion rate also increases in the presence of $CO_2$; on the other hand, just as can be seen from Fig.1, pH value of the solution in the absence of $Na_3PO_4$ is about 3.8 and that in the presence of $10^{-2}$ mol $L^{-1}$ $Na_3PO_4$ is about 4.4, which means that the exist formation of phosphate ion is $H_2PO_4^-$, furthermore, according to the pourbaix diagram of Mg, $Mg(OH)_2$ is unstable when pH value is lower than 8.5, thus insoluble $Mg_3(PO_4)_2$(s) and $Mg(OH)_2$(s) can not form in this solution, Heakal et al.[16] also pointed out that precipitation of $Mg_3(PO_4)_2$(s) and $Mg(OH)_2$(s) is impossible in acid solution. Therefore, here the role of phosphate ion is to act as electrolyte, with increasing the concentration of $Na_3PO_4$, the conductivity of solution increases, meaning that the anodic dissolution accelerates with increasing the concentration of $Na_3PO_4$. With hydrogen evolution going on, concentration of $H^+$ ions will decrease, and the pH value will increase. After the equilibrium pH value required for the precipitation of $Mg_3(PO_4)_2$(s) and $Mg(OH)_2$(s) meet the qualification, insoluble $Mg_3(PO_4)_2$(s) and $Mg(OH)_2$(s) will form on the anodic sites. In additional, the following reaction will take place:

$$2Mg^{2+}(aq)+2OH^-(aq)+CO_3^{2-}(aq)\rightarrow Mg_2(OH)_2CO_3(s) \qquad (9)$$

So with immersion time increased, the insoluble corrosion product $Mg_2(OH)_2CO_3$(s), $Mg_3(PO_4)_2$(s) and $Mg(OH)_2$(s) also increase and accumulate on the surface of AZ31B, which become thicker with time and have a high protective action. The formation of $Mg_2(OH)_2CO_3$(s), $Mg_3(PO_4)_2$(s) and $Mg(OH)_2$(s) further restricts the transport of $CO_2$ and $O_2$ to the magnesium surface and thereby favors the inhibitive effect with time increased. This is in agreement with the result obtained from effect of immersion time.

## 5. CONCLUSIONS

(1) In solution without $CO_2$, $Na_3PO_4$ can inhibit the corrosion of AZ31B magnesium alloy, the corrosion decreases with increasing $Na_3PO_4$ concentration, the anodic dissolution will go into passive zone with increasing the applied potential when the concentration is equal to or higher than $10^{-2}$ mol $L^{-1}$. However, in solution saturated with $CO_2$, $Na_3PO_4$ will accelerate the corrosion of AZ31B magnesium alloy, and the corrosion rate increases with increasing $Na_3PO_4$ concentration.

(2) $CO_2$ plays an important role in the corrosion of AZ31B magnesium alloy in $Na_3PO_4$ solution. The corrosion of AZ31B is stronger in $Na_3PO_4$ solution saturated with $CO_2$ than without $CO_2$. EIS shows that the corrosion reaction is controlled by charge transfer resistance and film resistance. The results of potentiodynamic polarization and EIS are consistent.

(3) The inhibitive effect of $CO_2$ is also observed with time increased due to hydrogen evolution which results in increase of the pH value, showing that $CO_2$ reduces the average corrosion rate due to the formation of insoluble products. With increase in immersion time, the protective film becomes thicker, the $i_{corr}$ decrease and $R_t$ increase.

ACKNOWLEDGEMENT

This work was supported by Natural science fund item of China under the Grant Number 51161025，Natural science fund item of Yunnan province under the Grant Number 2011FZ173, Department of Education fund item of Yunnan province under the Grant Number 2011Y211, Program for Innovative Research Team (in Science and Technology) in University of Yunnan Province (IRTSTYN) and Green Chemisty and Functional Materials Research for Yunnan Innovation Team under the Grant Number 2011HC008.

## References

1. W. Liu, F. Cao, L. Chang, Z. Zhang, J. Zhang, *Corros. Sci*. 51(2009)1334.
2. Y.H. Wei, L.J. Yang, L.F. Hou, Y.W. Guo B.S. Xu, *Eng. Fail. Anal*. 16(2009)19.
3. A.K. Mondal, S. Kumar, C. Blawert, N.B. Dahotre, *Surf. & Coa. Tech*. 202(2008)3187.
4. Z. Shi, G. Song, A. Atrens, *Corros. Sci*. 47(2005)2760.
5. P.B. Srinivasan, C. Blawert, W. Dietzet, K.U. Kainer, *Scripta Mater*. 59(2008)43.
6. R.L. Edgar, *Automotive Light Metals* 1(2000)42.
7. G.L. Markar, J. Kruger, *Int. Mater. Rev*. 38(1993)138.
8. G. Baril, N. Pébère, *Corros. Sci*. 43(2001)471.
9. C. Lin, X. Li, *Rare Metals* 25(2006)190.
10. R. Lindstrom, J. E. Svensson, L. G. Johansson, *J. Electrochem. Soc*. 149(2002) B103.
11. Q. Qu, J. Ma, L. Wang, L. Li, W. Bai, Z. Ding, *Corros. Sci*. 53(2011)1186.
12. Ž. Mesíková, P. Šulcová, M.Trojan, *J. Therm. Anal. Cal*. 88(2007)103.
13. G. Y. Li, J. S. Lian, L. Y. Niu, Z. H. Jiang, Q. Jiang, *Surf. Coat. Technol*. 201(2006) 1814
14. H. Hsiao, W. Tsai, *Surf. Coat. Technol*. 190(2005)299
15. L. Y. Niu, Z.H. Jiang, G. Y. Li, C.D. Gu, J.S. Lian, *Surf. Coat.Technol*. 200(2006)3021
16. F. El-Taib Heakal, A. M.Fekry, M. Z. Fatayerji, *J. Appl. Electrochem*. 39(2009)583.
17. G. Song, A. Atrens, D. ST Jonh, X. Wu, J. Nairn, *Corros. Sci*. 39(1997)1981.
18. G. Song, A.Aterens, X. Wu, B. Zhang, *Corros. Sci*. 40(1998)1769.
19. Q. Qu, S. Jiang, W. Bai, L. Li, *Electrochem. Acta*. 52(2007)6811.
20. Q. Qu, S. Jiang, L. Li, W. Bai, J. Zhou, *Corros. Sci*. 50(2008)35.
21. G. baril, C. Blanc, N. Pébère, *J. Electrochem. Soc*. 148(2001)B489.
22. L. Li, Q. Qu, Z. Fang , L.Wang, Y. He, R. Yuan, Z. Ding, *Int. J. Electrochem. Sci*., 7(2012)12690.
23. L. Larabi, Y. Harek, M. Traisnel, A. Mansri, *J. Appl. Electrochem*. 34(2004)833.
24. P. Bommersbach, C. Alemany-Dumont, J. P. Millet, B. Normand, *Electrochim. Acta*. 51(2006)4011.